vided one accounts for the sign of the imaginary part of either the zero or the polynomial appropriately.

In order to change the sign of the real part of $z$, it is noted that if $z$ were $|x| - j|y|$ (instead of $-|x| + j|y|$), the signs of the odd powers of $z$ would be changed, but those of the even powers would remain the same, By changing the sign of every odd power of $z$ by shifting the burden of the sign to the coefficient, the output of the adding circuit is as if $z$ were $|x| - j|y|$, which enables one to deal with plus values of $x$. The fact that the sign of the imaginary part is minus is unimportant, but of course the remarks above on conjugates must be regarded.

## VII. Conclusion

This paper describes an instrument for generating polynomials and for finding the roots, real or complex, of any polynomial, of any degree, with either real or complex coefficients, and to any degree of accuracy. It is also shown that this instrument may be built with commercially available parts.

# The Measurement of Current Distributions along Coupled Antennas and Folded Dipoles*

T. MORITA†, ASSOCIATE, IRE, AND C. E. FAFLICK†, STUDENT, IRE

*Summary*—**The theoretical analysis of coupled antennas is facilitated by the use of symmetrical and antisymmetrical currents. This paper presents experimental results verifying this physical concept of current on closely coupled antennas and folded dipoles.**

## I. Introduction

THE THEORETICAL ANALYSIS of coupled antennas is carried out advantageously by representing the current in each element as a superposition of symmetrical (codirectional) and antisymmetrical (oppositely directed) components of current.[1] If the spacing between the elements satisfies the near-zone conditions $\beta_0 b = 2\pi 1\lambda \ll 1$, the symmetrical components maintain the far-zone field and may therefore be called the radiating or antenna currents; while the antisymmetrical components which contribute insignificantly to the far-zone field are essentially nonradiating or transmission-line currents. It is the purpose of this paper to verify experimentally this physical concept of currents in coupled antennas and folded dipoles.

## II. Measuring Apparatus and Techniques

Fig. 1 is a block diagram of the measuring setup. The basic structure on which all current-distribution measurements were made consists of a coaxial line, the shield of which ends at a conducting ground plane; the extension of the inner conductor over the ground plane forms the antenna.[2] Protruding from a slot in the center conductor is a small shielded loop which can be moved along the entire length of the antenna and into the coaxial line to measure both the current distribution on the antenna and line and the standing-wave ratio on the line. In this way the impedance of the antenna is obtained. The length of the antenna may be increased by extending the inner conductor a greater distance over the plane by a rack-and-pinion movement. The second element of the coupled antenna is formed by a quarter-inch rod which is parallel to the slotted antenna and composed of threaded sections that may be adjusted in length to any integral number of centimeters. This element may be connected to or insulated from the ground plane; in the latter case the antenna is connected to a type-$N$ connector.

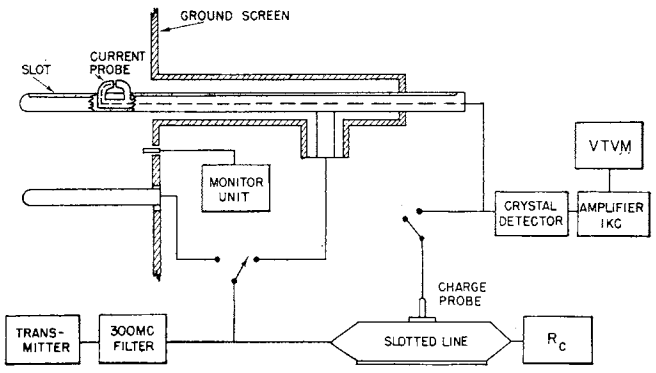


Fig. 1—Block diagram for measuring setup.

The problem is to use the same slotted antenna to measure the current distribution on both the driven and parasitic elements. By symmetry, the feed points may be interchanged so that the slotted antenna can be used as the parasitic antenna. A small charge probe, located symmetrically between the two elements, is used both as an amplitude and a phase-reference monitor so that when the two elements are interchanged,

* Decimal classification: R129×R142. Original manuscript received by the Institute, September 12, 1950; revised manuscript received, March 13, 1951.

The research reported in this paper was made possible through support extended Cruft Laboratory, Harvard University, by the Naval Department (ONR), the Signal Corps, the United States Army, and the United States Air Force, under ONR Contract N5ori-76, T. O. 1.

† Cruft Laboratory, Harvard University, Cambridge, Mass.

[1] King, Mimno, and Wing, "Transmission Lines, Antennas, and Waveguides," McGraw-Hill Book Co., New York, N. Y.; pp. 224–226; 1945.

[2] T. Morita, "Current distributions on transmitting and receiving antennas," PROC. I.R.E., vol. 38, pp. 898–904; August, 1950.

the relative amplitudes and phases of the currents on each element may be determined.

Relative phase is measured by adding the signal from the test probe to a signal obtained from a traveling probe on a slotted line terminated in its characteristic impedance. All measurements were made at 300 mc, modulated by a 1-kc signal. A 1N21B crystal and a tuned amplifier were used in the detector circuit and the voltage was read on a Ballantine vacuum-tube voltmeter.

To measure the current distribution on a folded dipole, a short-circuiting bar was placed at the ends of the coupled antennas described above. Measurements were made for coupled antennas and folded dipoles of lengths $h=\lambda/4$ and $\lambda/2$ with spacing between elements of $b=0.04\lambda$.

## III. Resolution of Measured Distribution into Symmetrical and Antisymmetrical Currents

By application of the superposition theorem it is always possible to solve the problem of two coupled

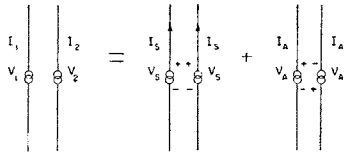

Fig. 2—Resolution of measured distribution into symmetrical and antisymmetrical currents.

antennas, center-driven by voltages $V_1$ and $V_2$, by obtaining the solutions for symmetrically and antisymmetrically driven pairs. From Fig. 2 it follows that

$$V_1 = \tfrac{1}{2}(V_S + V_A)$$
$$V_2 = \tfrac{1}{2}(V_S - V_A),$$

or

$$V_S = V_1 + V_2$$
$$V_A = V_1 - V_2.$$

Similarly,

$$I_1 = \tfrac{1}{2}(I_S + I_A)$$
$$I_2 = \tfrac{1}{2}(I_S - I_A),$$

or

$$I_S = I_1 + I_2 \tag{1}$$
$$I_A = I_1 - I_2,$$

and

$$Z_1 = \frac{V_1}{I_1}. \tag{2}$$

For the particular case under consideration, the second element is parasitic. Thus,

$$V_2 = 0,$$

or

$$V_S = V_A,$$

and

$$V_1 = \tfrac{1}{2}V_S,$$

so that

$$Z_1 = \frac{2V_S}{I_S + I_A} = \frac{2Z_AZ_S}{Z_A + Z_S},$$

with

$$Z_S = \frac{V_S}{I_S} \tag{3}$$

and

$$Z_A = \frac{V_A}{I_A}.$$

In measuring, the impedance of the antenna with its coupled element, as well as the relative amplitudes and relative phases of the currents in the elements, has been obtained. It is desirable to secure the absolute amplitudes and absolute phases of the measured distributions. If $V_1$ is arbitrarily chosen to be 1 volt, with a phase angle of 0 degrees, it follows from (2) that

$$|I|\,\underline{|-\theta^0} = \frac{1\,\underline{|0^\circ}}{|Z_1|\,\underline{|\theta^\circ}}.$$

Therefore, the reciprocal of $Z_1$ gives the amplitude of current in amperes per volt, while the negative of the phase angle of the impedance gives the phase angle of the current at the gap. This establishes the absolute value of amplitude in amps per volt, and the phase of the current at any point.

With such a procedure it may be assumed that it is possible to define a unique voltage at the gap. From the point of view of the wave picture, the electromagnetic field at the gap can be represented in terms of the dominant TEM mode in the coaxial line, together with nonpropagating higher-order modes introduced at the gap, in order to satisfy the boundary condition at the discontinuity. The assumption of a voltage of $1\,\underline{|0^\circ}$ volt at the gap from measurements on the line is equivalent to neglecting these higher-order modes and representing the driving voltage only in terms of the dominant TEM mode. Theoretically, this means that the voltage assigned to the gap is actually the voltage defined back in the line, one wavelength from the gap, where only the dominant mode is present. By application of (1), the symmetrical and antisymmetrical components of current may be obtained. The symmetrical and antisymmetrical impedances may be derived from (3). Moreover, the mutual and self-impedances $Z_{12}$ and $Z_{11}$ are given by the following:

$$Z_{12} = Z_{21} = \tfrac{1}{2}(Z_S - Z_A)$$

and

$$Z_{11} = \tfrac{1}{2}(Z_S + Z_A).$$

## IV. Results

### *A. Coupled Antennas*

In Figs. 3 and 5 are shown the measured distributions of the magnitudes and phases of the currents on both the driven and parasitic elements of two coupled antennas, for which $\beta_0 h = \pi/2$ and $\pi$. By following the procedure developed in the foregoing section, these currents are decomposed into the symmetrical and antisymmetrical components of Figs. 4 and 6. The antisymmetrical currents may be identified with the equal and opposite currents of a two-wire transmission line. Since the symmetrical currents are equal and in phase in both elements, they may be identified with the radiating or antenna currents.

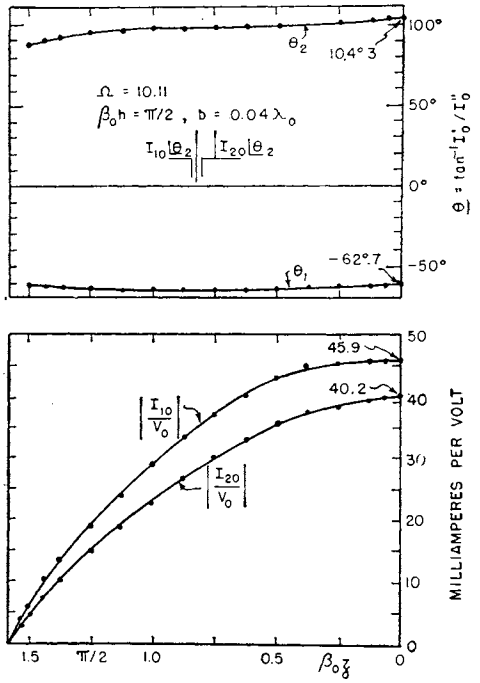


Fig. 3—Measured current distribution on coupled antenna, $h=\lambda/4$, $b=0.04\lambda$.

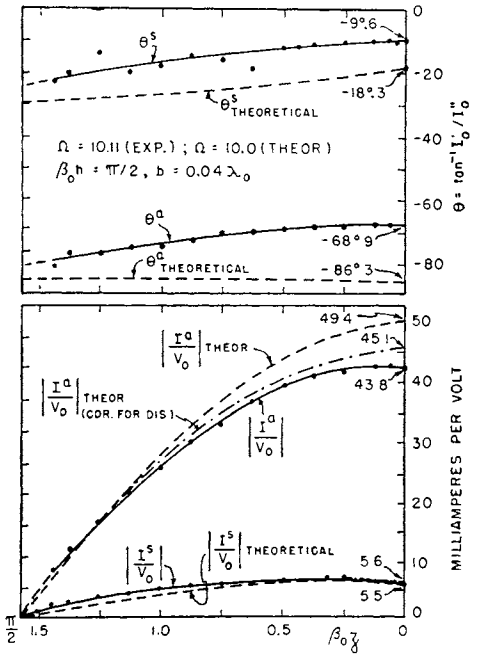


Fig. 4—Symmetrical and antisymmetrical components for coupled antenna, $h=\lambda/4$, $b=0.04\lambda$.

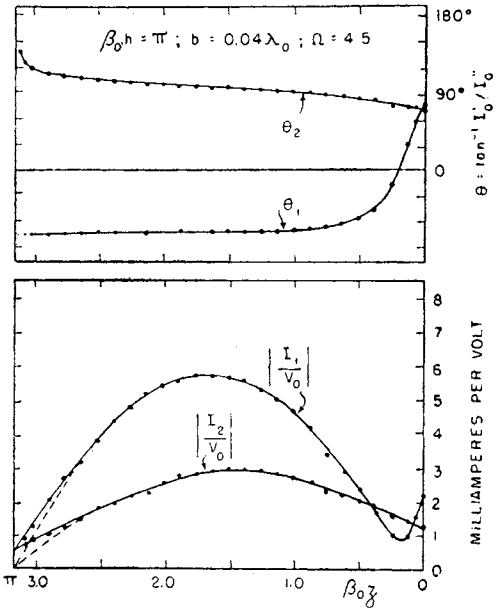


Fig. 5—Measured current on coupled antenna, $h=\lambda/2$, $b=0.04\lambda$.

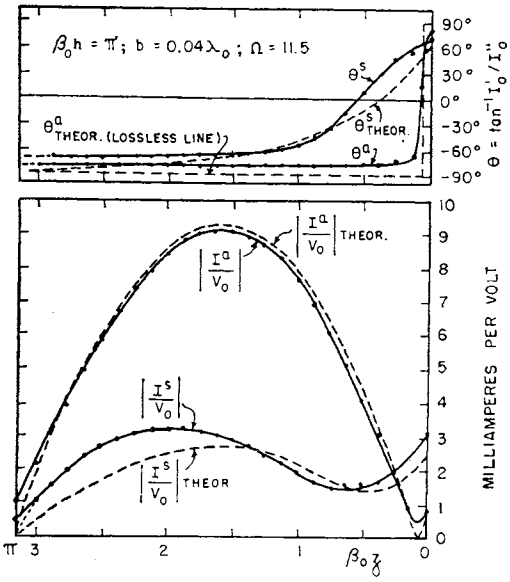


Fig. 6—Symmetrical and antisymmetrical currents for coupled antennas, $h=\lambda/2$, $b=0.04\lambda$.

It is interesting to compare the large amplitude of the antisymmetrical current with that of the symmetrical current. Since antisymmetrical components do not radiate, it is obvious that the antisymmetrical component has the effect of lowering the efficiency of the antenna if the transmission line has ohmic losses. Note that

TABLE I

| $\beta_0 h = \frac{\pi}{2}$ | *Experimental* $\Omega = 10.11 = 2 \log \frac{2h}{a}$ | *Theoretical No Ohmic Dissipation* $\Omega = 10$ | *Theoretical with Added Series Resistance of 3.55Ω to Compensate for Ohmic Dissipation* |
|---|---|---|---|
| $Z_1$ | $10.0+j19.2=21.8 \angle 62.7^0$ | $3.2+j19.0=19.3 \angle 80.5^0$ | $9.3+j17.9=20.2 \angle 62.5^0$ |
| $Z_{11}=Z_{22}$ | $45.8+j12.8=47.6 \angle 15.6^0$ | $42+j19.3=46.3 \angle 24.6^0$ | $45.6+j19.3=49.5 \angle 22.9^0$ |
| $Z_{12}$ | $41.6+j\ 1.9=41.7 \angle 2.6^0$ | $41.4+j\ 9.2=42.3 \angle 12.4^0$ | $41.4+j\ 9.15=42.3 \angle 12.4^0$ |
| $Z_S$ | $87.4+j14.7=88.6 \angle 9.4^0$ | $83.4+j28.4=88.1 \angle 18.8^0$ | $86.95+j28.4=91.4 \angle 18.1^0$ |
| $Z_A$ | $4.2+j10.9=11.7 \angle 68.9^0$ | $0.65+j10.1=15.5 \angle 86.3^0$ | $4.2+j10.1=11.0 \angle 67.4^0$ |
| $\beta_0 h = \pi$ | $\Omega = 11.3$ | $\Omega = 10$ | |
| $Z_1$ | $122-j454$ | $170-j352$ | |
| $Z_{11}=Z_{22}$ | $127-j782$ | $52.5-j987$ | |
| $Z_{12}$ | $-43+j494$ | $52.5+j798$ | |
| $Z_S$ | $84.5-j289$ | $105-j190$ | |
| $Z_A$ | $170-j1275$ | $0-j1785$ | |

for $\beta_0 h = \pi$, the distances between minimum amplitudes are smaller for the symmetrical current distribution than for the antisymmetrical distribution. Theoretical curves[3,4] are shown for the symmetrical currents computed from the second-order solution to the integral equation; the antisymmetrical currents are compared with the sinusoidal distribution characteristic of a lossless transmission line.[3] In the theoretical formulation it is assumed that the antenna is driven by a difference of scalar potential applied by a ring generator, while the experimental model is driven by a coaxial line over an image plane. Since these methods of driving are equivalent only in the physically unavailable limit of a coaxial line with a dielectric of vanishingly small radius and a comparably small gap, only qualitative agreement is to be expected.

It is interesting to note that for $\beta h = \pi/2$ much better agreement with the experimental value is obtained if 3.55 Ω is added in series with the theoretical antisymmetrical resistance in Table I (above), to correct for the ohmic dissipation.

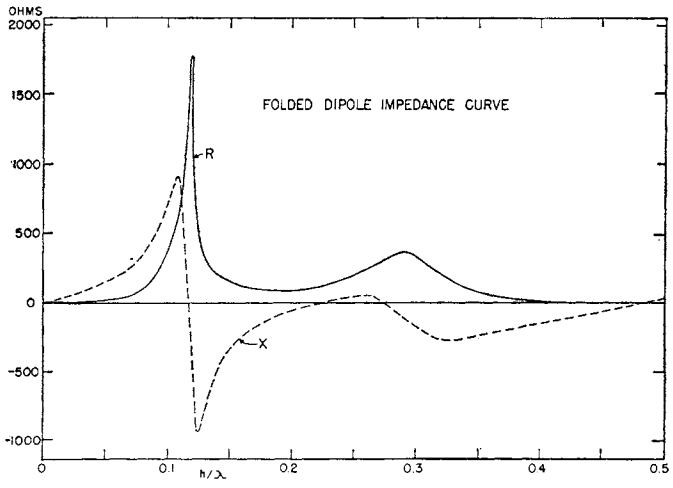


Fig. 7—Measured impedance for folded dipole, $b = 0.04\lambda$.

[3] C. T. Tai, "The theory of coupled antennas and its applications," PROC. I.R.E., vol. 36, pp. 487–497; April, 1948.

[4] R. W. P. King, "Self- and Mutual Impedances of Parallel Identical Antennas," Cruft Laboratory Technical Report No. 118, Harvard University, Cambridge, Mass.; November, 15, 1950.

### B. Folded Dipole

In Fig. 7 are shown the measured curves of resistance and reactance as a function of the length of the folded dipole over an image plane. The region of broad-band behavior for this structure is between points of antiresonance. For studying the behavior of the folded dipole in this range, a value of $\beta_0 h = \pi/2$ was selected. The measured distribution curve is shown in Fig. 8, and the symmetrical and antisymmetrical components in Fig. 9. The symmetrical components has a maximum at the gap while the antisymmetrical current has a maximum at the end of the antenna. The antisymmetrical current is the same as that of a short-circuited transmission line of length $l = h + b/2$, where $b$ is the spacing between the two conductors.

A clearer picture of this concept of symmetrical and antisymmetrical currents may be obtained from a study of the phase diagram in Fig. 10. Here the voltage of the gap is taken as $1 \angle 0^\circ$ volts. Since the antenna is slightly

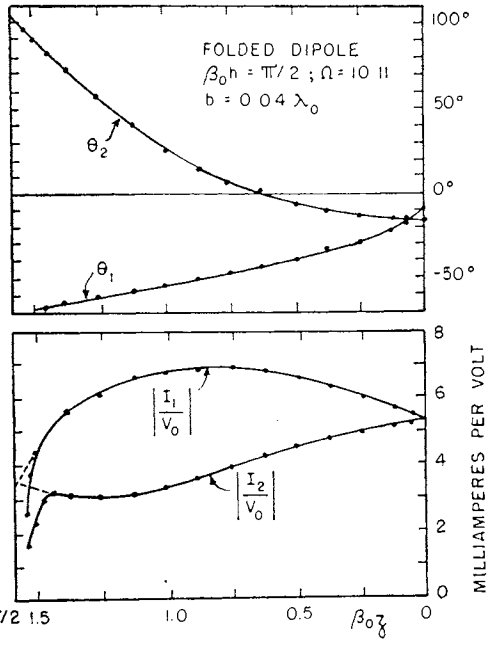


Fig. 8—Measured current on folded dipole, $h = \lambda/4$, $b = 0.04\lambda$.

longer than the resonant length of a dipole, the impedance for the symmetrical component is slightly inductive and small. Accordingly, the symmetrical current at the gap is large and lags behind the voltage by

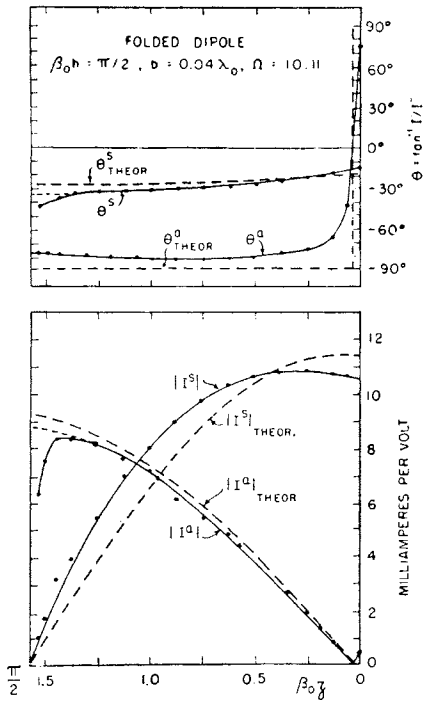


Fig. 9—Symmetrical and antisymmetrical components for folded dipole, $h=\lambda/4$.

a small angle. As we proceed along the antenna, the current amplitude decreases, falling to zero at the end, while the phase lags by a small amount as the end is approached, causing the phasor to rotate clockwise.

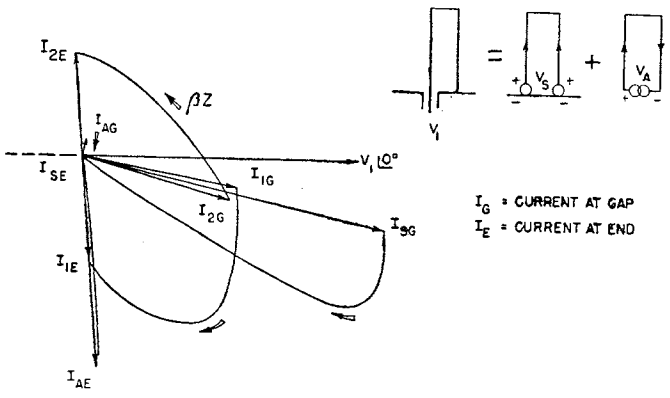


Fig. 10—Vector diagram for current distribution on folded dipole, $h=\lambda/4$.

Since the equivalent short-circuited transmission line is slightly longer than a quarter wavelength, the antisymmetrical impedance is high and capacitive. This means that the antisymmetrical current is small and leads the applied voltage by nearly 90 degrees at the gap. At the quarter wavelength from the end, phase reversal takes place, with the antisymmetrical current going to a minimum. Beyond this point the current increases sinusoidally, reaching a maximum at the short-circuited termination. The vector sum and difference of the symmetrical and antisymmetrical currents give the currents on the driven and parasitic elements, respectively. For this case the following impedances are obtained:

*Experimental*

$$Z_1 = 188 + j36.4$$
$$Z_{11} = 513 - j116.9$$
$$Z_{12} = -467 + j128.1$$
$$Z_S = 92.2 + j22.4$$
$$Z_A = 1{,}980 - j450.$$

In Fig. 11 we see the measured current distribution along a folded dipole, with $\beta_0 h = \pi$. Here the antisymmetrical current distribution is seen to be very much greater than the symmetrical current; hence, no reasonably accurate decomposition into symmetrical and antisymmetrical currents is possible.

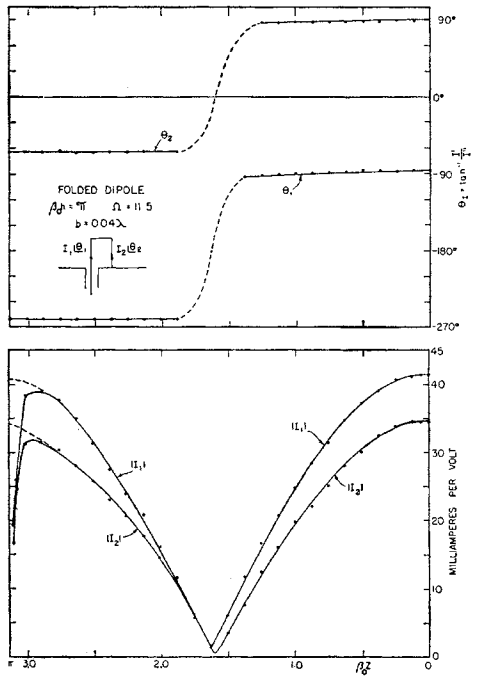


Fig. 11—Measured current on folded dipole, $h=\lambda/2$, $b=0.04\lambda$.

## V. Conclusion

A method has been developed for measuring and interpreting distributions of current along both folded and parasitic dipoles. The results of the measurements have been compared with the theory, and qualitative agreement has been obtained. This is another illustration of the use of the concept of symmetrical and antisymmetrical components in physical problems.

## Acknowledgments

The authors are indebted to R. W. P. King of the Cruft Laboratory, Harvard University, for his guidance in the work, and to Mrs. R. Dressler, who did part of the computing.